

Insulin-like growth factor-1 short-period therapy improves non-alcoholic fatty liver disease in obese mice

Daniela C. Andrade,^{1*} Filipe Jorge Nascimento,¹ Genilza P. de Oliveira,¹ Thiago Freire,¹ Simone N. de Carvalho,¹ Ana Carolina Stumbo,¹ Laís Carvalho,¹ Alessandra A. Thole,¹ Erika Cortez¹

Abstract

This study seeks to evaluate Insulin-like Growth Factor 1 (IGF-1) short-period therapy in Non-Alcoholic Fatty Liver Disease (NAFLD) as it relates to western diet-induced obesity. For this purpose, 21-day-old male Swiss mice were divided into a control group (CG, N=8), which was fed a standard diet, and an obese group (GO, N=16), which was fed a western diet, rich in saturated fat and simple carbohydrates, for 12 weeks. In the 11th week, part of the animals in the obese group (N=8) received a daily subcutaneous injection of recombinant human IGF-1 (100µg/kg/day) during seven consecutive days (GO+IGF-1). Biometric and metabolic parameters, intraperitoneal glucose tolerance test (IGTT), quantitative analysis of liver steatosis, quantitative analysis of collagen in liver and expression of immunoperoxidase of alpha-smooth muscle actin (α-SMA) were analyzed. Our data demonstrated that IGF-1 short-term treatment was able to improve

1. Laboratório de Pesquisa em células-tronco. Departamento de Histologia e Embriologia. Instituto de Biologia. Universidade do Estado do Rio de Janeiro. Rio de Janeiro, RJ, Brazil.

*Correspondence address:

E-mail: daniela.caldas.andrade@gmail.com

ORCID: <https://orcid.org/0000-0002-7907-9342>

BJHBS, Rio de Janeiro, 2023;22(2):81-90

DOI: 10.12957/bjhbs.2023.79959

Received on 22/03/2023. Approved on 03/09/2023.

obesity-related biometric and metabolic parameters. In addition, it promoted the recovery of liver parenchyma, thereby reducing steatosis and fibrosis, thus demonstrating an important hepatoprotective action.

Keywords: Non-Alcoholic Fatty Liver Disease; Liver Fibrosis; IGF-1; Obesity.

Introduction

Despite its multifactorial nature, obesity is deeply related to nutritional habits, including the consumption of foods with high calorie content, rich in saturated fat, salt and sugar, usually called the western diet.^{1,2} In addition to an increase in fat deposits, obesity is linked to comorbidities, including type 2 diabetes mellitus (T2DM), nonalcoholic fatty liver disease (NAFLD), hypertension, hyperlipidemia, chronic kidney disease, and cardiovascular disease, leading to increased mortality in obese individuals.³

Non-alcoholic fatty liver disease (NAFLD) is one of the most prevalent chronic liver conditions and an important risk factor for liver cirrhosis and hepatocellular carcinoma.⁴ NAFLD is the spectrum of liver disease in which hepatic steatosis, the macrovesicle accumulation of triglyceride in hepatocytes,^{5,6} is considered the ultimate effector of lipotoxic liver injury.⁷

Insulin-like growth factor-1 (IGF-1) is an anabolic growth hormone associated with proliferation, growth and cellular metabolism, and low IGF-1 plasma levels have been correlated with obesity^{8,9} and NAFLD.¹⁰ Therefore, this study sought to investigate the therapeutic potential of short-period of recombinant IGF-1 treatment on NAFLD in an experimental model of obesity induced by the western diet.

Methods

Animals and experimental design

Animals were cared for in accordance with the guidelines of the Ethics Commission on Animal Use of the Biology Institute of the State University of Rio de Janeiro (CEUA/026/2017), established under standard international protocols.

Male Swiss mice at the 21st day after birth were housed under standard conditions of temperature and controlled humidity with a 12h light/dark cycle. Animals were randomly divided into a control group (CG, N=8), which was fed a standard AIN93G diet (65.6% carbohydrates, 17.3% proteins, and 17.1% lipids) and an obese group (OG=16), which was fed a Western diet rich in saturated fat and simple carbohydrate from clarified butter (ghee) (43.3% carbohydrates, 14% proteins, and 42.7% lipids) (PragSoluções, Brazil).

Diets were administered during 12 weeks with free access to water and food. After 11 weeks, half of the obese group mice (N=8) received a daily subcutaneous injection of 50µl of human recombinant IGF-1 (100µg.kg⁻¹.day⁻¹) (PeproTech) in saline solution for seven consecutive days (OG+IGF-1). The other groups received injections of 50µl of phosphate buffer saline.

Biometric and metabolic parameters

Body weight and naso-anal length were assessed after 12 weeks, and the Lee index was calculated by the formula: cube root of body weight (g)/naso-anal length (cm)×1,000. Epididymal and retroperitoneal fat were excised and weighed. In addition, the liver steatosis index was analyzed by liver mass (g)/body mass (g). Fasting glucose was measured with a glucometer (Accu-Chek Active, Roche Diagnostics, Germany) on the euthanasia day (111th day of life) and fasting insulin was evaluated by radioimmunoassay (Insulin IRMA KIT; ref. IM3210, Beckman Coulter, Miami). The Homeostasis Model Assessment of Insulin Resistance (HOMA-IR) index was calculated by using the formula: [fasting insulin (µUI/mL)×fasting glucose (mmol/L)]/22.5.

Intraperitoneal glucose tolerance test (IGTT)

Intraperitoneal glucose tolerance test was performed after 6 hours of fasting after 12 weeks of diet. An intraperitoneal injection of glucose (1g/kg of body weight) was administered, and blood droplets were collected from the tail vein just prior to glucose administration (time 0) and after 30, 60, 90 and 120 minutes. The blood glucose level was measured using a glucometer and AccuChek Active test strips (Roche Diagnostics, Germany).

Quantitative analysis of liver steatosis

The liver was fixed in 4% formaldehyde, and paraffin sections were stained with hematoxylin and eosin. To quantify liver fat droplets, 15 random fields per animal, collected from non-serial

sections, were captured in a light microscope with CCD camera. The analysis was conducted with STEPanizer software. Results were expressed as density/area (μm^2).

Quantitative analysis of collagen in liver

The liver was collected, fixed in 4% paraformaldehyde, dehydrated in increasing series of alcohol, clarified in xylol, and included in paraffin. Sections of $5.0\mu\text{m}$ were obtained and stained with Picro-Sirius Red (0.1% solution of Direct Red 80, Sigma-Aldrich), which stains collagen fibers in red, and hematoxylin. To quantify hepatic collagen deposition, 15 random fields per animal, collected from non-serial sections, were captured with a 40x objective in a light microscope with CCD camera. The analysis was made with Image Pro Plus 3.0 software by densitometry of areas stained in red. The results were expressed as a percentage of stained area over the total field.

Immunoperoxidase of alpha-smooth muscle actin (a-SMA)

The liver was fixed in 4% formaldehyde and included in paraffin. Sections were then incubated with monoclonal mouse anti-rat alpha-smooth muscle actin primary antibody (Santa Cruz Biotechnology), followed by anti-mouse biotinylated secondary antibody, streptavidin-peroxidase and, finally, DAB chromogen. The sections were then stained with hematoxylin and mounted with Entellan. To quantify a-SMA expression in the experimental groups, 15 random fields per animal were captured in a light microscope with a CCD camera and then analyzed with Image Pro Plus 3.0 software.

Statistical analysis

Data were expressed as mean \pm standard error of the mean and statistical significance was assessed by one-way or two-way analysis of variance with Holm-Sidak post-test, with $P\leq 0.05$ being considered statistically significant.

Results

Biometric and metabolic parameters

From week 5 of western diet administration, the OG demonstrated a significant increase in body mass compared to the CG ($P<0.0001$), which persisted until the end of the experiment (Figure 1A). However, the OG + IGF-1 showed 15% of body mass reduction compared to the OG group, reaching values similar to the CG (Table 1).

After IGF-1 treatment, the values of Lee index, epididymal fat, and retroperitoneal fat mass similar to the CG were also restored in the OG+IGF-1, with no difference in naso-anal length between groups. In addition, the OG+IGF-1 showed a 13% of reduction in the steatosis hepatic index when compared to the OG group (Table 1).

IGF-1 treatment improved fasting glycemia compared to the OG, although it did not fall to the levels seen in the CG. Moreover, only one week of treatment was not enough to improve insulin levels and HOMA-IR (Table 1).

IGTT analysis demonstrated that the OG showed an almost two-fold increase in glucose intolerance compared to the CG. After IGF-1 treatment, the OG+GF-1 showed an improvement in the glucose tolerance curve (-22%) compared to the OG (Figure 1C-D).

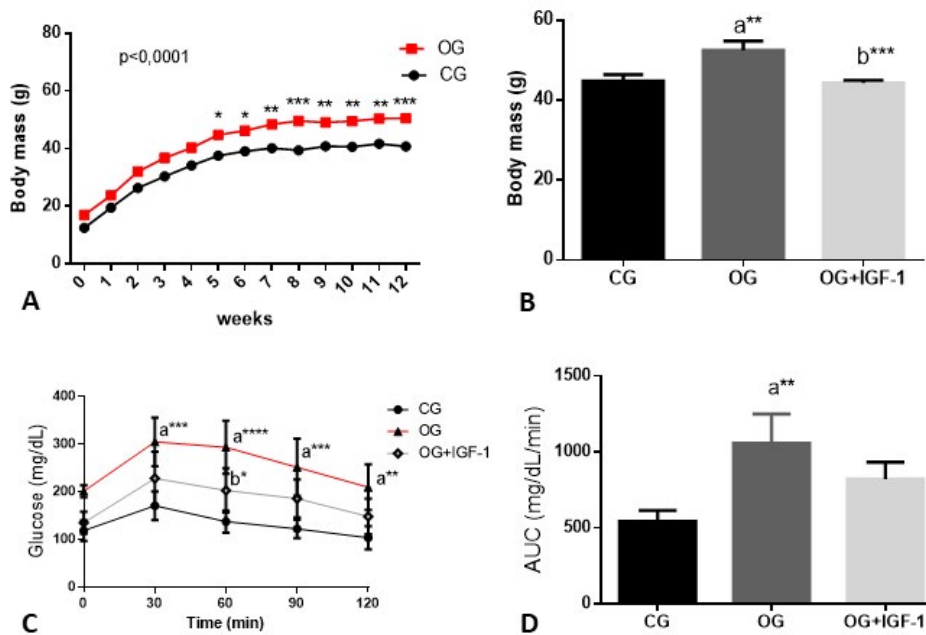


Figure 1. Body mass evolution, Intra-peritoneal glucose tolerance test and Area under the curve

Legend: (A) Body mass evolution of the control group (CG) and the obese group (OG) for 12 weeks. P value of change in time using repeated measures model effect. (B) Body mass on the day of euthanasia of CG, OG, and OG + IGF-1. (C) Intra-peritoneal glucose tolerance test. P value of change in time using repeated-measures model effect. (D) Area under the curve. Data are expressed as mean ± SEM. “a” significant difference compared to CG, “b” significant difference compared to OG. *P < 0.05; **P < 0.01; ***P < 0.001; ****P < 0.0001.

Source: The authors (2022).

Table 1. Biometric and metabolic parameters

	CG	OG	OG+IGF-1
Body mass (g)	44,7±1,6	52,4± 2,3 ^a	44,3±0,6 ^b
Naso-anal length (cm)	8,9±0,2	9,4±0,1	9,3±0,1
Lee Index	346,5±4,48	419,5±3,53 ^a	318,6±13,53 ^b
Fasting blood glucose (mg/dL)	102,8±9,4	175,0±5,3 ^a	139,8±9,4 ^{a,b}
Epididymal fat (g)	0,82±0,1	2,24±0,3 ^a	1,32±0,1 ^b
Retroperitoneal fat (g)	0,30±0,06	0,91±0,12 ^a	0,52±0,06 ^b
Insulin levels (mUI/mL)	50±8,4	124,3±5,7 ^a	159±19,2 ^a
HOMA-IR	2,18±0,3	4,71±0,6 ^a	4,96±0,62 ^a
Liver Steatosis (g/g)	0,04110±0,00094	0,05131±0,00283 ^a	0,04451±0,00124 ^b

Legend: Data are expressed as mean ± SEM; n = 8/group. a: Significant difference compared to CG. b Significant difference compared to OG. *P < 0.04; **P < 0.0019; ***P < 0.0005; ****P < 0.0001

Source: The authors (2023).

Steatosis quantification

The light microscopy analysis of liver sections stained with hematoxylin and eosin (Figure 2) showed that hepatic parenchyma of the OG has an intense degree of steatosis. Both macrovesicular (large vacuoles within each hepatocyte, which make the nucleus eccentric) and microvesicular (despite numerous vacuoles within each cell, the nucleus remains in its central position) steatosis was observed. However, the predominance of macrovesicular steatosis is evident. The OG+IGF-1 showed a significant improvement of the hepatic parenchyma, with an almost total reduction of macrovesicular steatosis; however, some hepatocytes with microvesicular steatosis remained. The quantification of fat droplets demonstrated that the OG (1097 ± 135.5) presented a significant increase in fat droplets per area in relation to the CG (321.9 ± 80.75). IGF-1 treatment was able to reduce hepatic steatosis by 43.4% in the GO+IGF-1 (621.3 ± 53.32) compared to the GO (Figure 2D).

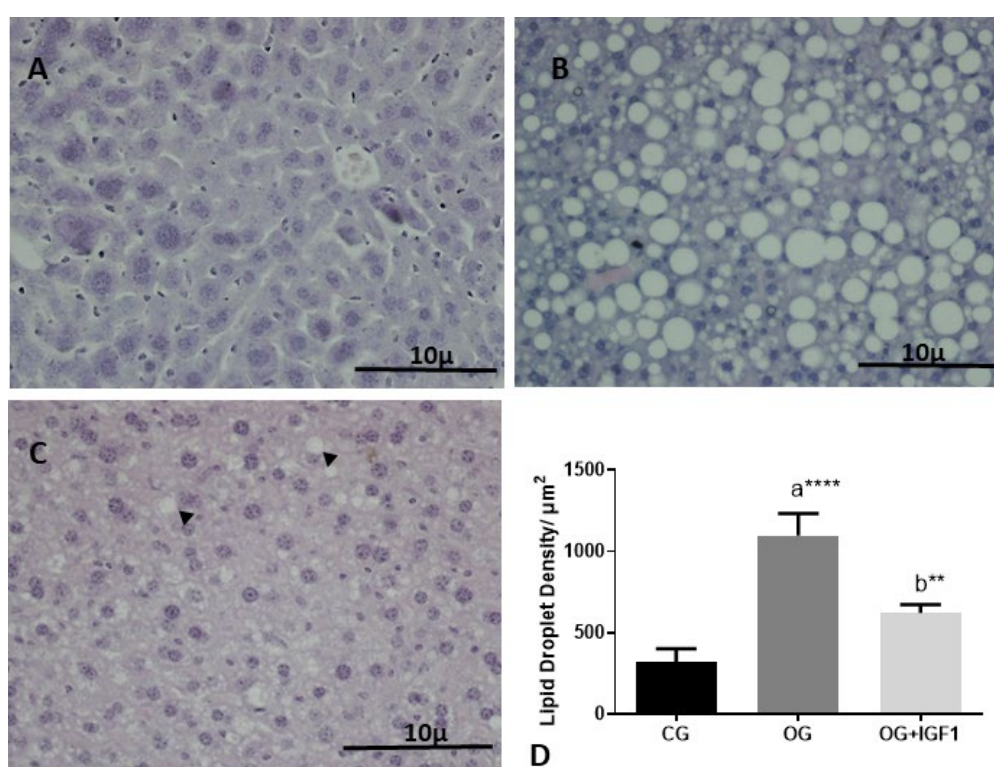


Figure 2. Histological liver sections stained with Hematoxylin and Eosin from (A) CG (control group), (B) OG (obese group) and (C) OG + IGF-1. (D) Quantitative analyses of Lipid Droplet Density/ μm².

Legend: Data are expressed as mean ± SEM. Arrowhead indicate hepatocytes with microvesicular steatosis. "a" significant difference compared to CG, "b" significant difference compared to OG. ** P < 0.0015 ****P < 0.0001.

Source: The authors (2023).

Liver fibrosis quantification

Picro Sirius Red staining demonstrated that collagen deposition in the liver was higher in the OG (Figure 3B) than the CG (Figure 3A). Treatment with IGF-1 reduced the fibrosis area by 43% compared to the OG (Figure 3D).

For fibrosis analysis, liver sections were stained with Picro-Sirius Red, which shows collagen deposition allowing the quantification of these areas. Compared to the CG (Figure 3A), the OG

showed greater deposition of collagen in the hepatic parenchyma, mainly around the vessels and between the hepatocyte cords (perisinusoidal area) (Figure 3B). In contrast, the OG+IGF-1 demonstrated a decrease in collagen deposition, which was mainly restricted to the area around the vessels, like the CG.

Quantitative analysis of Picro-Sirius Red stained area corroborated microscopic analysis that showed a significant increase of 30% in collagen deposition in the OG compared to the CG, characterizing the adverse remodeling of the extracellular matrix. However, after IGF-1 treatment, a significant reduction of 43% occurred in the fibrosis area compared to GO (Figure 3D).

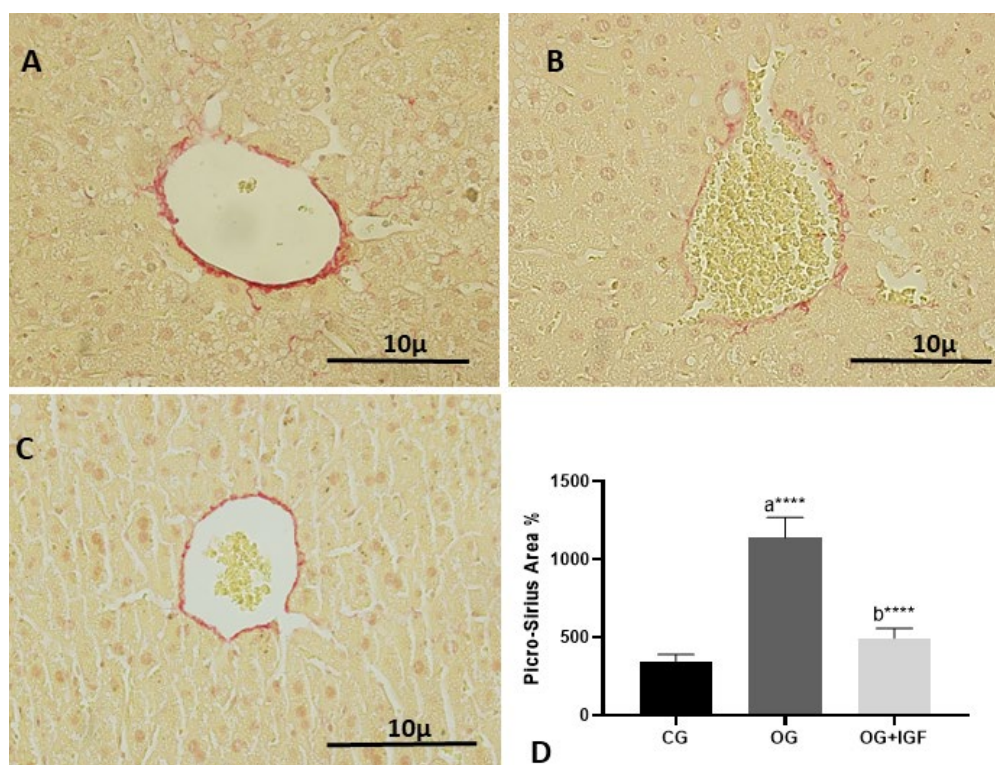


Figure 3. Histological liver sections stained with PicroSirius Red from (A) CG (control group), (B) OG (obese group) and (C) OG + IGF-1. (D) Quantitative analyses of PicroSirius stained area (D)

Legend: Data are expressed as mean \pm SEM. "a" significant difference compared to CG, "b" significant difference compared to OG. ****P < 0.0001

Source: The authors (2023).

Immunoperoxidase of α -SMA

Analysis of α -SMA expression in the liver demonstrated that this biomarker of activated myofibroblast has an extremely low expression in the CG (Figure 4A). However, the OG showed increased α -SMA expression between hepatocyte cords and around the centrilobular vein (Figure 4B). After a short period of IGF-1 treatment, hepatic parenchyma of OG+IGF-1 demonstrated an evident decrease in the α -SMA expression (Figure 4C).

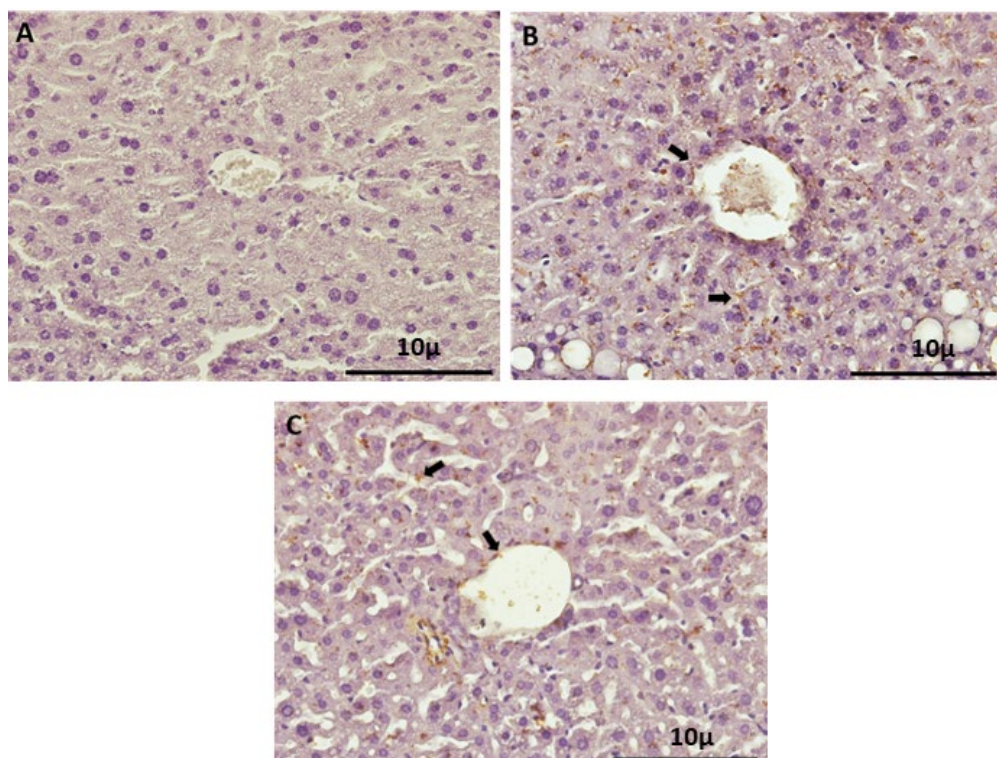


Figure 4. Histological heart sections immunostained with the smooth muscle alpha-actin-specific antibody, showing its staining in brown (arrows) and nuclei counterstained with hematoxylin, in purple.

Legend: (A) CG (control group); (B) OG (obese group) (C) OG + IGF-1.

Source: The authors (2023).

Discussion

The nutritional profile of the global population has been changing in recent decades with an increasing consumption of ultra-processed foods, with a high content of simple carbohydrates and saturated fat (western diet). Consequently, we observe an increase in caloric consumption at the expense of its expenditure, which results in alarming rates of obesity. In this study, we reproduced this dietary pattern, using the model described by Tikellis and colleagues² in male Swiss mice, already used by our group for some years,^{11,12} in order to evaluate the therapeutic potential of IGF-1 in NAFLD induced by western diet on the restructuring of the liver parenchyma.

The present study corroborated the obesogenic character of the western diet showed by our previous studies, which found increases in body mass, adiposity and glycemia.^{11,12} IGF-1-treated mice even showed a significant reduction in body mass after only one week of treatment, presenting the same body mass as the CG. IGF-1 activates the (PI3K)/Akt pathway, leading to anabolic effects and increasing lean mass through protein synthesis.^{11,13} It also promotes an increase in lipid oxidation and inhibition of lipogenesis, preventing generation of new adipocytes,¹⁴ which explains the reduction in adiposity in the treated group.

Obesity resulting from the excessive increase of calorie consumption in the western diet promotes the deposit of fat in the liver, leading to hepatic steatosis. Consequently, fatty acids accumulate in hepatocytes, resulting in a state of lipid cell hypertrophy. The excessive concentration of intracellular lipid in the hepatocyte causes steatosis, giving the hepatic parenchyma two distinct histological characteristics. In the first, microvesicular, the cytoplasm of the he-

patocyte is affected by small lipid vacuoles and the nucleus is located in the center of the cell. On the other hand, the macrovesicular steatosis is characterized by large vacuoles filled with lipids throughout the cytoplasm with consequent restriction of the nucleus to the periphery of the cell.¹⁵

For steatosis evaluation, we initially estimated hepatic steatosis, measured by the correction of liver weight (g) by the body mass (g), which showed a significant increase in the OG ratio when compared with the CG, indicating enlargement of the liver caused by fat accumulation. However, the OG+IGF-1 displayed a decrease in liver mass. To corroborate these initial results, the liver parenchyma was analyzed by light microscopy. We observed a significant amount of lipid droplets throughout the hepatic parenchyma of the OG, which is characteristic of hepatic steatosis, both microvesicle and macrovesicle. However, animals treated with IGF-1 for only one week showed a decrease in the density of lipid droplets, which were reduced to some regions of microvesicle hepatic steatosis, which demonstrated an improvement in the liver parenchyma of the mice. Nishizawa and colleagues¹⁶ in a mouse model with GH deficiencies (SDR), revealed that these mice presented hepatic steatosis, hepatic fibrosis and increased oxidative stress according to NAFLD phenotype. In this model, however, treatment for four weeks with either GH or IGF-1 was sufficient to reverse the phenotype, with IGF-1 infusion having a particularly beneficial effect on fibrosis compared with GH infusion.

Liver steatosis promotes a lipotoxic environment characterized by oxidative stress, lipid peroxidation, mitochondrial dysfunction and extensive hepatocellular death.¹⁷ Kupffer cells lead to an inflammatory phenotype and secretion of inflammatory cytokines, such as IL-6, TNF- α and IL-1 β . In addition to Kupffer cells, other immune cells are recruited into the tissue, contributing to the inflammatory profile.¹⁸ In this context, sinusoidal cells, as well as resident and recruited immune cells, secrete pro-fibrotic factors, such as TGF- β and reactive oxygen species (ROS).¹⁹ Such events stimulate fibrogenesis, since they activate the hepatic stellate cells, responsible for the deposition of extracellular matrix, altering the liver parenchyma and liver functionality.^{20,21}

Hepatic stellate cells immune-activated by cell infiltration and liver injury undergo a phenotypic transdifferentiation, and start to express actin smooth muscle (α -SMA).²² and to produce an extracellular matrix component, such as I, III and IV.^{18,23} The accumulation of collagen is accompanied by an imbalance between the consequences of tissue matrix metalloproteinases (MMPs) and tissue inhibitors of metalloproteinases (TIMPs). In murine fibrotic hybrids, the increase in MMPs was accompanied by an increase in TIMP-1.²⁴ This creates a direction for fibrogenesis in the MMP/TIMP balance with a shift in MEC synthesis and therefore fibrogenesis.²⁵

Our results corroborated findings that the western diet promotes liver fibrosis in NAFLD patients and showed an increased fibrotic area in the OG²⁶. After a single week of treatment, we observed reduced fibrosis in the hepatic parenchyma. In vitro experimental model reports an IL-6 decreasing in HepG2 cells, indicating the anti-inflammatory effect of IGF-1,²⁷ also demonstrated in mice CCl₄ model, such as reducing oxidative stress and liver fibrosis,²⁸ through activation of the AKT pathway, which our group observed in previous work on the heart.¹¹

Our data showed greater collagen deposition in the areas close to the portal triad, around the central-lobular vein and in the perisinusoidal spaces, which coincided with the area marked by α -SMA, an activated HSC marker (myofibroblast) in the OG. These results indicate that the western diet triggered a lipotoxic inflammation responsible for the activation of the fi-

brogenic profile of hepatic stellate cells. The OG+IGF-1, after a short-term treatment, showed a significant reduction of hepatic fibrosis area, indicating the hepatoprotective action of IGF-1.

A NAFLD study model, using db/db mice fed a methionine-choline-deficient diet treated with IGF-1, showed a reduction in pro-fibrotic markers, such as procollagen 1a1 and collagen 4a1, and inflammatory markers, such as Il-1 β and Il-6, by PCR. In addition the number of α -SMA positive cells was reduced, indicating a direct effect of IGF-1 on activated hepatic stellate cells that would promote their senescence, assessed by β -galactosidase activity both in vivo and in vitro. IGF-1 also promoted the increase of Mmp9 and a reduction of Timp1, thereby helping to resolve the fibrosis.²⁹

Another study, which used transgenic mouse models (SMP8-IGF-I) to induce a cirrhotic state with carbon tetrachloride (CCl₄), showed that SMP8-IGF-I mice exhibited decreased α -SMA expression and morphological improvement of the hepatic parenchyma, which restricts the activation of hepatic stellate cells and decreases fibrogenesis.³⁰ These data confirm our results, in which treatment with IGF-1 is related to a lower expression of α -SMA in the hepatocyte cords, which promotes the improvement of the liver.

Conclusion

Short-term treatment with IGF-1 was effective for the recovery of hepatic parenchyma in obese mice, which contributes to the improvement of NAFLD and represents a promising therapeutic approach.

Financial support

This work was supported by the Fundação Carlos Chagas Filho de Amparo à Pesquisa do Rio de Janeiro (FAPERJ) and the Conselho Nacional de Desenvolvimento Científico e Tecnológico (CNPq).

Conflict of interest

The authors declare that they have no conflict of interest in this study.

Ethical standards

All experimental procedures were approved by the Animal Care and Use Committee of the Biology Institute of the State University of Rio de Janeiro (CEUA 002/2017) and comply with the principles contained in Brazilian Law no. 11.794/2008.

References

1. Popkin BM. Contemporary nutritional transition: determinants of diet and its impact on body composition. *Proc Nutr Soc.* 2011 Feb;70(1):82-91. doi: 10.1017/S0029665110003903. Epub 2010 Nov 22. PMID: 21092363; PMCID: PMC3029493.
2. Tikellis C, Thomas MC, Harcourt BE, et al. Cardiac inflammation associated with a Western diet is mediated via activation of RAGE by AGEs. *Am J Physiol Endocrinol Metab.* 2008 Aug;295(2):E323-30. doi: 10.1152/ajpendo.00024.2008. Epub 2008 May 13. PMID: 18477705; PMCID: PMC2652498.
3. Global BMIMC, Di Angelantonio E, Bhupathiraju Sh N, et al. Body-mass index and all-cause mortality: individual-participant-data meta-analysis of 239 prospective studies in four continents. *Lancet* 2016;388:776–86.
4. Marques V, Afonso MB, Bierig N, et al. Adiponectin, Leptin, and IGF-1 are useful diagnostic and stratification biomarkers of NAFLD. *Front Med (Lausanne).* 2021 Jun 23;8:683250. doi: 10.3389/fmed.2021.683250. PMID: 34249975; PMCID: PMC8260936.
5. Chalasani N, Younossi Z, Lavine JE, et al. The diagnosis and management of nonalcoholic fatty liver disease: practice guidance from the American Association for the Study of Liver Diseases.
6. Sheka AC, Adeyi O, Thompson J, et al. Nonalcoholic Steatohepatitis: A Review. *JAMA.* 2020 Mar 24;323(12):1175-1183. doi: 10.1001/jama.2020.2298. Erratum in: *JAMA.* 2020 Apr 28;323(16):1619. PMID: 32207804.
7. Wang DQ, Portincasa P, Neuschwander-Tetri BA. Steatosis in the liver. *Compr Physiol.* 2013 Oct;3(4):1493-532. doi: 10.1002/cphy.c130001. PMID: 24265237.
8. Berryman DE, Glad CA, List EO, et al. The GH/IGF-1 axis in obesity: pathophysiology and therapeutic considerations. *Nat Rev Endocrinol.* 2013 Jun;9(6):346-56. doi: 10.1038/nrendo.2013.64. Epub 2013 Apr 9. PMID: 23568441.
9. Ren J, Anversa P. The insulin-like growth factor I system: physiological and pathophysiological implication in cardiovascular diseases associated with metabolic syndrome. *Biochem Pharmacol.* 2015 Feb 15;93(4):409-17. doi:

- 10.1016/j.bcp.2014.12.006. Epub 2014 Dec 23. PMID: 25541285.
10. Arturi F, Succurro E, Procopio C, et al. Nonalcoholic fatty liver disease is associated with low circulating levels of insulin-like growth factor-I. *J Clin Endocrinol Metab.* 2011 Oct;96(10):E1640-4. doi: 10.1210/jc.2011-1227. Epub 2011 Aug 3. PMID: 21816784.
 11. Andrade D, Oliveira G, Menezes L, et al. Insulin-like growth factor-1 short-period therapy improves cardiomyopathy stimulating cardiac progenitor cells survival in obese mice. *Nutr Metab Cardiovasc Dis.* 2020 Jan 3;30(1):151-161. doi: 10.1016/j.numecd.2019.09.001. Epub 2019 Sep 9. PMID: 31753790.
 12. de Oliveira GP, de Andrade DC, Nascimento ALR. Insulin-like growth factor-1 short-period therapy stimulates bone marrow cells in obese Swiss mice. *Cell Tissue Res.* 2021 Jun;384(3):721-734. doi: 10.1007/s00441-020-03357-9. Epub 2021 May 11. PMID: 33977324.
 13. Vitale G, Pellegrino G, Vollery M, et al. ROLE of IGF-1 System in the modulation of longevity: controversies and new insights from a centenarians' perspective. *Front Endocrinol (Lausanne).* 2019 Feb 1;10:27. doi: 10.3389/fendo.2019.00027. PMID: 30774624; PMCID: PMC6367275.
 14. Liu JL. Does IGF-I stimulate pancreatic islet cell growth? *Cell Biochem Biophys.* 2007;48(2-3):115-25. doi: 10.1007/s12013-007-0016-7. PMID: 17709881.
 15. Takahashi Y, Soejima Y, Fukusato T. Animal models of non-alcoholic fatty liver disease/nonalcoholic steatohepatitis. *World J Gastroenterol.* 2012;18(19):2300-2308. <https://doi.org/10.3748/wjg.v18.i19.2300>
 16. Nishizawa H, Takahashi M, Fukuoka H, et al. GH-independent IGF-I action is essential to prevent the development of nonalcoholic steatohepatitis in a GH-deficient rat model. *Biochem Biophys Res Commun.* 2012 Jun 29;423(2):295-300. doi: 10.1016/j.bbrc.2012.05.115. Epub 2012 May 30. PMID: 22659415.
 17. Del Campo JA, Gallego P, Grande L. Role of inflammatory response in liver diseases: Therapeutic strategies. *World J Hepatol.* 2018 Jan 27;10(1):1-7. doi: 10.4254/wjh.v10.i1.1. PMID: 29399273; PMCID: PMC5787673.
 18. Heyens LJM, Busschots D, Koek GH, et al. Liver fibrosis in non-alcoholic fatty liver disease: from liver biopsy to non-invasive biomarkers in diagnosis and treatment. *Front Med (Lausanne).* 2021 Apr 14;8:615978. doi: 10.3389/fmed.2021.615978. PMID: 33937277; PMCID: PMC8079659.
 19. Wahid B, Ali A, Rafique S, et al. Role of altered immune cells in liver diseases: a review. *Gastroenterol Hepatol.* 2018 Jun-Jul;41(6):377-388. English, Spanish. doi: 10.1016/j.gastrohep.2018.01.014. Epub 2018 Mar 28. PMID: 29605453.
 20. Weiskirchen R, Weiskirchen S, Tacke F. Recent advances in understanding liver fibrosis: bridging basic science and individualized treatment concepts. *F1000Res.* 2018 Jun 27;7:F1000 Faculty Rev-921. doi: 10.12688/f1000research.14841.1. PMID: 30002817; PMCID: PMC6024236.
 21. Buzzetti E, Pinzani M, Tsochatzis EA. The multiple-hit pathogenesis of non-alcoholic fatty liver disease (NAFLD). *Metabolism.* 2016 Aug;65(8):1038-48. doi: 10.1016/j.metabol.2015.12.012. Epub 2016 Jan 4. PMID: 26823198.
 22. Higashi T, Friedman SL, Hoshida Y. Hepatic stellate cells as key target in liver fibrosis. *Adv Drug Deliv Rev.* 2017 Nov 1;121:27-42. doi: 10.1016/j.addr.2017.05.007. Epub 2017 May 12. PMID: 28506744; PMCID: PMC5682243.
 23. Ramzy MM, Abdelghany HM, Zenhom NM, et al. Effect of histone deacetylase inhibitor on epithelial-mesenchymal transition of liver fibrosis. *IUBMB Life.* 2018 Jun;70(6):511-518. doi: 10.1002/iub.1742. Epub 2018 Mar 30. PMID: 29601129.
 24. Yoshiji H, Kuriyama S, Miyamoto Y, et al. Tissue inhibitor of metalloproteinases-1 promotes liver fibrosis development in a transgenic mouse model. *Hepatology.* 2000 Dec;32(6):1248-54. doi: 10.1053/jhep.2000.20521. PMID: 11093731.
 25. Roeb E, Purucker E, Breuer B, et al. TIMP expression in toxic and cholestatic liver injury in rat. *J Hepatol.* 1997 Sep;27(3):535-44. doi: 10.1016/s0168-8278(97)80359-5. PMID: 9314132.
 26. Soleimani D, Ranjbar G, Rezvani R, et al. Dietary patterns in relation to hepatic fibrosis among patients with nonalcoholic fatty liver disease. *Diabetes Metab Syndr Obes.* 2019 Mar 12;12:315-324. doi: 10.2147/DMSO.S198744. PMID: 30881075; PMCID: PMC6420105.
 27. Hribal ML, Procopio T, Petta S, et al. Insulin-like growth factor-I, inflammatory proteins, and fibrosis in subjects with nonalcoholic fatty liver disease. *J Clin Endocrinol Metab.* 2013 Feb;98(2):E304-8. doi: 10.1210/jc.2012-3290. Epub 2013 Jan 11. PMID: 23316084.
 28. Luo X, Jiang X, Li J, et al. Insulin-like growth factor-1 attenuates oxidative stress-induced hepatocyte premature senescence in liver fibrogenesis via regulating nuclear p53-progerin interaction. *Cell Death Dis.* 2019 Jun 6;10(6):451. doi: 10.1038/s41419-019-1670-6. PMID: 31171766; PMCID: PMC6554350.
 29. Nishizawa H, Iguchi G, Fukuoka H, et al. IGF-I induces senescence of hepatic stellate cells and limits fibrosis in a p53-dependent manner. *Sci Rep.* 2016 Oct 10;6:34605. doi: 10.1038/srep34605. PMID: 27721459; PMCID: PMC5056388.
 30. Sanz S, Pucilowska JB, Liu S, et al. Expression of insulin-like growth factor I by activated hepatic stellate cells reduces fibrogenesis and enhances regeneration after liver injury. *Gut.* 2005 Jan;54(1):134-41. doi: 10.1136/gut.2003.024505. PMID: 15591519; PMCID: PMC1774353.